ACS OMEGA

Article

Cite This: ACS Omega 2019, 4, 3627−3634

http://pubs.acs.org/journal/acsodf

Interaction Force Fluctuations in Antigen−Antibody Biorecognition Studied by Atomic Force Spectroscopy

Anna Rita Bizzarri,*[,†] Attila Gergely Végh,[‡] György Váró,[‡] and Salvatore Cannistraro[†]

[†]Biophysics and Nanoscience Centre, DEB, Università della Tuscia, Largo dell'Università, 01100 Viterbo, Italy

[‡]Institute of Biophysics, Biological Research Centre, Hungarian Academy of Sciences, Temesvári Krt. 62, H-6726 Szeged, Hungary

ABSTRACT: The formation of a specific complex between $\beta_2\mu$globulin and anti$\beta_2\mu$globulin was investigated by analyzing the force fluctuations recorded in an atomic force spectroscopy biorecognition experiment. We found that a $1/f$ noise appears in the power spectra of force fluctuations when the tip, functionalized with $\beta_2\mu$globulin, reaches a distance of 0.50 nm from the partner-charged substrate while a specific biorecognition process occurs. Concomitantly, in this active region, the distribution of the times spent by the tip in the proximity of the substrate exhibits a power law trend characterized by a long-time tail. All of these findings are put into relationship to a slowing down of the energy landscape exploration, consistent with a restricted sampling dynamics of the conformational states driving to the final binding state. The hypothesis that a combination of a conformational substrate and an induced fit hybrid binding mechanism controls the specific complex formation is put forward and discussed also in connection with the fluctuations of the hydration water network.

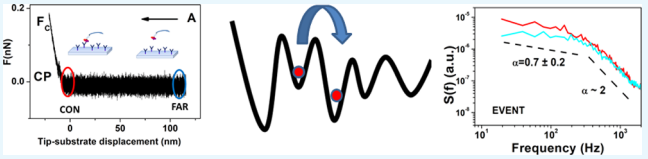

1. INTRODUCTION

Biological functions proceed through appropriate molecular interactions that take place by spanning a wide range of temporal scales.[1,2] These processes, collectively named biorecognition, involve several steps, which promote and regulate the approach and orientation of partners, giving rise to a final biomolecular complex. From a physical point of view, biorecognition can be seen as a diffusion along the hypersurface energy landscape, with trapping and escape from several local minima and[3] with such a picture being reminiscent of the conformational substrate model describing protein dynamics.[4,5] In this framework, two different mechanisms of the ligand−target binding have been proposed: conformational selection (CS)[3] and induced fit (IF).[6] Both mechanisms assume a two-step reaction in which a conformational transition of the target either precedes (CS) or follows (IF) the binding step with the ligand. In the former, the target exists in distinct conformations (corresponding to nearly isoenergetic local minima of the energy landscape) and the ligand selects the one with an optimal fit. In the latter, the conformation of the target changes after ligand binding to provide an optimal fit. These two models have long been considered as mutually exclusive, even if the possibility that they can coexist has recently been taken into consideration.[7] Sorting out the contribution of these mechanisms to any binding interaction remains a challenging task of general interest in biochemistry, biology, and biophysics. On the other hand, understanding biorecognition mechanisms deserves a high potentiality in applicative fields, such as the development and control of biosensors and drug designing.

Remarkable tools to investigate biorecognition rely on single-molecule techniques, which make accessible the study of even subtle biomolecular interaction details, usually hidden in ensemble measurements.[8,9] Among these techniques, atomic force spectroscopy (AFS) allows one to follow, at nearly physiological conditions, individual biomolecular partners during their approach, eventually forming a specific complex.[10,11] Furthermore, careful analysis of the applied forces causing unbinding of the complex provides information on a number of important complex-related parameters, such as the interaction strength, dissociation rate, affinity, and energy landscape features.[12] To this end, however, the forces should be carefully scrutinized to be unambiguously attributed to specific complex-unbinding events and not to unspecific ones, such as adhesion, trapping, and so on. A preliminary discrimination is generally achieved by analyzing the stretching of molecular linkers suitably introduced in the functionalization procedure.[13] Recently, we have proposed an alternative method to single out force curves corresponding to a specific biorecognition event on the basis of the appearance of a $1/f$ noise in the AFS force fluctuations recorded during the tip−substrate approaching stage.[14,15] This peculiar noise figure, which has been observed also in the ultrasensitive detection of biomolecules by a field-effect transistor,[16] represents a fingerprint of the occurrence of a specific complex formation.[15]

From a more general point of view, the presence of the $1/f$ noise in biorecognition force fluctuations is indicative of the physical complexity of the underlying mechanisms and suggests that AFS data may encode a larger amount of information on the biorecognition process.[14] Indeed, the $1/f$ noise can be put into relationship to the searching process of the molecular partners in the multiminimum hypersurface

Received: October 29, 2018
Accepted: December 26, 2018
Published: February 18, 2019

DOI: 10.1021/acsomega.8b02993
ACS Omega 2019, 4, 3627−3634

energy landscape, allowing us to address the exploration of the energy landscape and likely to discriminate between the CS or IF binding mechanisms.

With this aim, we have revisited the force fluctuation data recorded in an AFS biorecognition experiment during the approaching of two biomolecular partners undergoing a specific complex formation. We have used a closed-loop AFM equipment, able to monitor the effective distance between the tip and the substrate during the quasi-static approach of the partners, to record the force fluctuations at high sampling rate. We have chosen the complex formed between $\beta_2\mu$globulin and anti$\beta_2\mu$globulin, which had been previously investigated by our group using AFM imaging and AFS.[17] $\beta_2\mu$globulin is involved in the human immune system, and its level can be also used as a tumor marker.[18,19] A fluctuation-based analysis of force curves recorded in AFS biorecognition experiments on the $\beta_2\mu$globulin−anti$\beta_2\mu$globulin complex has put into evidence that the $1/f$ noise appears at a tip−substrate distance of about 0.50 nm. Concomitantly, it is found that the distribution of the times that the tip spends in the proximity of the substrate exhibits a power law trend characterized by a long-time tail. These results, which are a clear fingerprint of a complex behavior, could be put into relationship to a slowing down of the energy landscape exploration, consistent with a restricted sampling dynamics of the conformational states driving to the final binding state. The hypothesis that a combination of a conformational substrate (CS) and an induced fit (IF) hybrid binding mechanism is controlling the specific complex formation is put forward and discussed also in connection with the fluctuations of the hydration water network.

2. RESULTS AND DISCUSSION

The biorecognition experiment by AFS on the $\beta2\mu$globulin/anti$\beta2\mu$globulin complex has been carried out by vertically approaching an atomic force microscopy tip, functionalized with $\beta2\mu$globulin and put at the end of a cantilever, toward a substrate charged with anti$\beta2\mu$globulin. After reaching a fixed value of the maximum contact force, F_C, the approaching stage is stopped and the tip is retracted from the substrate. The force, which is proportional to the cantilever deflection, is recorded as a function of the effective tip−substrate distance (see Figure 1). The approaching curves have been acquired at a very low speed, in quasi-static conditions, and at a very high sampling rate. A representative approaching curve is shown in Figure 1A and reveals the occurrence of wide force fluctuations around a zero value up to the contact point (CP), at which a physical contact between the functionalized tip and the substrate is reached. Beyond that point, the repulsive forces between the tip and the substrate yield an upward deflection of the cantilever, whereas the fluctuations become much less evident. As usually detected in AFS experiments, all of the approaching curves appear very similar among them. At variance, the retraction curves generally match the trace of the approaching ones up to the contact point, but the curves may exhibit different trends beyond the contact point, depending on the specific features of the tip−substrate interaction. In particular, they may follow the same trend as in the approaching phase, as shown in the inset of Figure 1B, with this being indicative that no significant interaction between the tip and the substrate has occurred. Alternatively, they may show a linear or nonlinear downward deflection, followed by a jump-off to the baseline, corresponding to a detachment of the tip from the substrate. A linear trend is generally attributed to nonspecific adhesions between the tip and the substrate, without any specific interaction between the biomolecules. At variance, a nonlinear trend might be due to the unbinding of the complex, eventually formed during the approaching stage. In this case, the jump-off provides information on the unbinding force of the specific complex, whose analysis, in the framework of suitable theoretical models, allows us to determine important complex-related parameters, such as interaction strength, dissociation rate, etc. (for a wider description of curves in AFS biorecognition experiments, see ref 12). However, force curves showing a nonlinear trend in the retraction stage might not be related to specific unbinding events and further analyses are required to single out those curves effectively corresponding to a specific biorecognition event. A common procedure consists in the checking for the stretching of the molecular linker (e.g., poly(ethylene glycol), PEG) before unbinding.[12,13] As already mentioned, we have developed an alternative method on the basis of the appearance of $1/f$ noise on force fluctuations.[14,15] Here, we have applied such a method to select 30 force curves related to specific biorecognition events; for comparison, 30 curves related to nonspecific events have been also taken into consideration (see the Experimental Section).

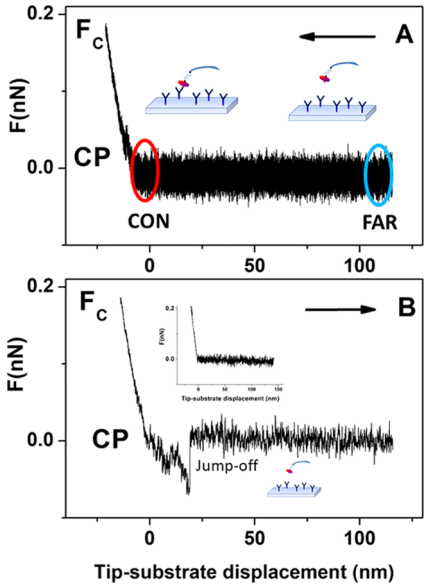

Figure 1. Representative force curves from an AFS experiment carried out with a tip functionalized with $\beta_2\mu$globulin toward a glass substrate covered with anti$\beta_2\mu$globulin. (A) Approaching curve, recorded at a speed of 10 nm/s; 10 nm long regions at the beginning (azure circle) and just before the contact point (red circle) are marked. (B) Retraction curve, recorded at a speed of 1000 nm/s related to a specific biorecognition event. Inset: retraction force curve with no event. CP: contact point; F_C: maximum contact force.

Accordingly, we have focused our attention to the 10 nm long region of the approaching curve, located (i) at the initial part of the curve (azure circle in Figure 1A), named the FAR region, and (ii) before the contact point (red circle in Figure 1A), named the CON region. Figure 2 shows an example of both these regions related to specific (Figure 2A,B) and nonspecific (Figure 2C,D) unbinding events. In all of the cases, we note fast fluctuations overimposed on slower fluctuations, with no significant differences at visual inspection.

DOI: 10.1021/acsomega.8b02993
ACS Omega 2019, 4, 3627−3634

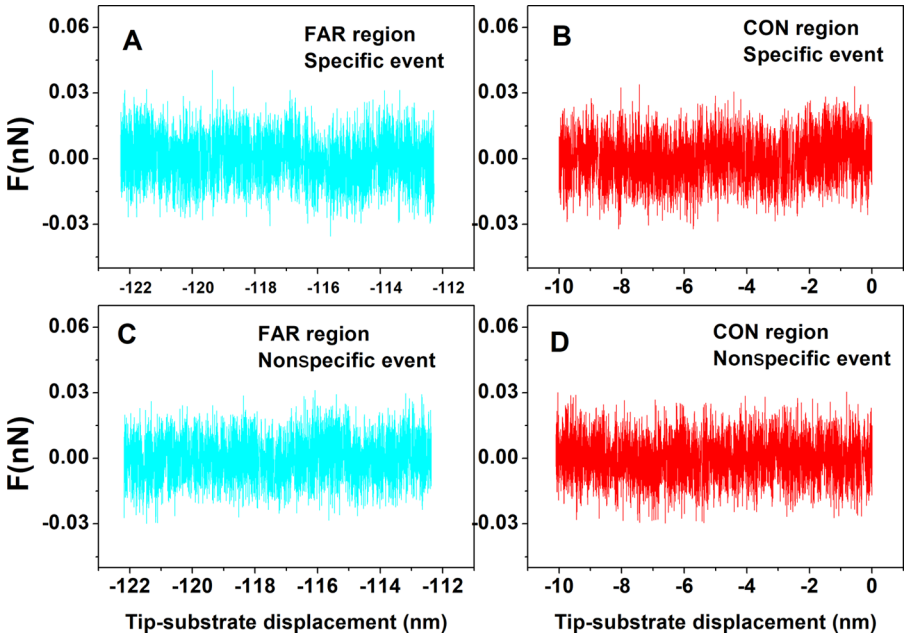

Figure 2. Zoom of the 10 nm long regions from the approaching curves, located at the beginning (A and C, azure curves) and just before the contact point (B and D, red curves); data is related to both specific and nonspecific events (see also Figure 1).

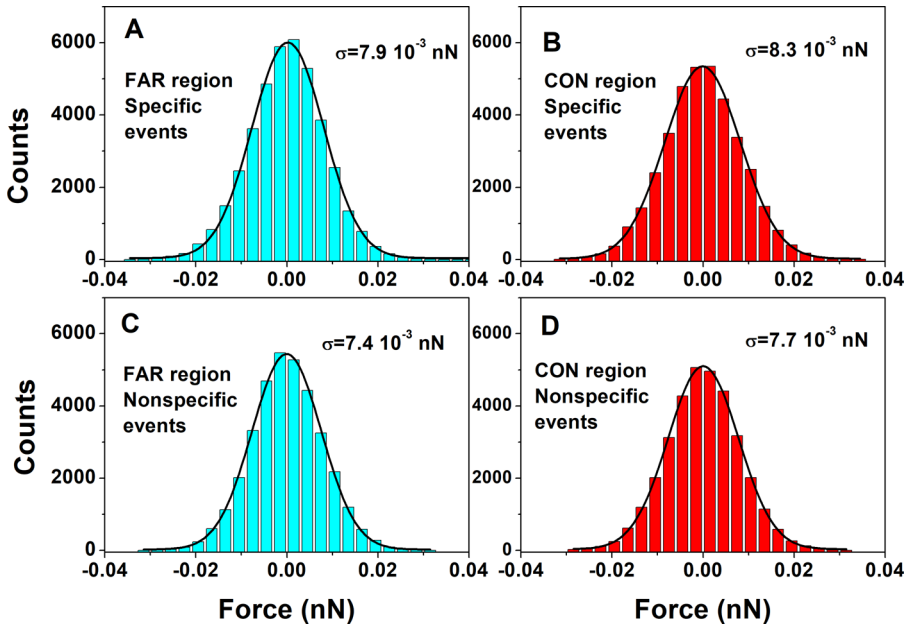

Figure 3. Histograms of the force amplitude of the 10 nm long regions from the approaching curve at the beginning (A and C, azure columns) and just before the contact point (B and D, red columns); data is related to both specific and nonspecific events. Continuous black lines are the fitting curves by a Gaussian function; the corresponding standard deviation values are reported.

The histograms of the force amplitude detected in these regions are representatively shown in Figure 3. All of the histograms are characterized by a single-mode distribution centered at about 0 and well-described by a Gaussian function (see black lines in Figure 3). Slightly wider distributions, as witnessed by the higher standard deviation values, are detected for the CON region with respect to FAR regions; similar trends have been observed for histograms from all of the curves.

Generally, the force fluctuations in an AFS biorecognition experiment can be ascribed to several causes, such as thermally induced fluctuations, high-frequency fluctuations from the force feedback system, mechanical vibrations, drift effects, etc., together with a possible contribution from the tip−substrate interactions.[14,20] The latter contribution is expected to become progressively more significant as far as the tip approaches the contact point, in agreement with that observed in our data.

The spectral content of FAR and CON regions has been analyzed by calculating the power spectrum as described in the Experimental Section; representative power spectra from curves related to both specific and nonspecific events are shown in Figure 4. In the log−log plot, all of the spectra are characterized by two different linear regimes, separated by a cutoff frequency of about 300 Hz. Accordingly, each regime

DOI: 10.1021/acsomega.8b02993
ACS Omega 2019, 4, 3627−3634

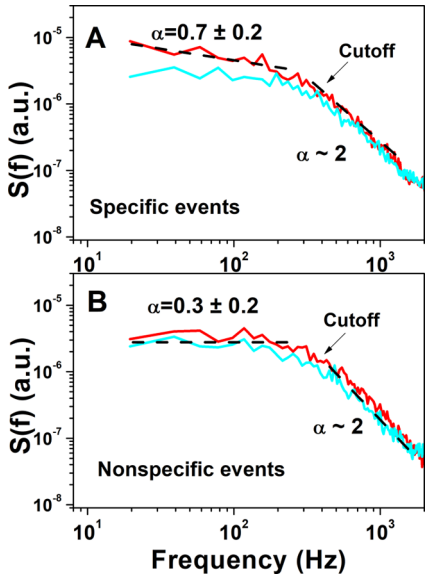

Figure 4. Power spectra of 10 nm long regions from the approaching curves located at the beginning (azure curves) and just before the contact point (red curves), for both specific (A) and nonspecific (B) events. Dashed black lines are the best fit through the expression $S(f) \sim 1/f^{\alpha}$, below and above the cutoff frequency detected at about 300 Hz. The reported α exponents are the average and the corresponding standard deviation as obtained from a collection of 30 curves.

can be fitted by an expression given as $P \sim 1/f^{\alpha}$ with the corresponding α exponent providing information about the system. At frequencies higher than the cutoff, all of the spectra exhibit almost the same slope with an α value close to 2 (i.e., $P \sim 1/f^2$), which is indicative of the so-called red noise, corresponding to a constant correlation function. Red noise can reflect thermally driven fluctuations, without any special distinctive role in regulating processes. At frequencies below the cutoff, the power spectra of all of the FAR and CON regions from nonspecific events are almost flat ($P \sim$ constant) and an α exponent close to 0 ($\alpha = 0.3 \pm 0.2$) has been extracted. At variance, the power spectra of the CON regions related to specific events are still linear but with an α exponent close to 1 ($\alpha = 0.7 \pm 0.2$). These α values related to the low-frequency power spectra from curves attributed to nonspecific and specific events have been statistically compared by a confidence test. We found that they are significantly different at a level higher than 90%. Accordingly, the power spectra of curves related to nonspecific events are characterized by white noise, whereas curves attributed to specific biorecognition events reveal the presence of $1/f$ noise.

The appearance of $1/f$ noise in the 10 nm long region before the contact point can be then put into relationship to the occurrence of a specific biorecognition process, as demonstrated in our previous works.[14,15] We remark that the $1/f$ noise, or flickering noise, generally reflects a complex temporal behavior,[21] in systems characterized by multiple time scale processes. Indeed, the $1/f$ noise has been traced back to the trapping/escaping in/from local minima of a rough energy landscape explored by the system.[22] In this respect, we note that a cutoff frequency of about 300 Hz indicates that the biorecognition process involves temporal processes whose characteristic times are lower than about 3 ms (see below). On the other hand, the cutoff frequency is lower than that previously found (~3−5 kHz),[14,15] likely due to the much lower approaching speed, allowing a much higher temporal resolution.

To localize the region where the $1/f$ noise is established, we have calculated the power spectra using 0.25 nm long intervals, progressively sampled along the 10 nm long region and globally exhibiting $1/f$ noise. Again, we have found that all of the spectra are characterized by two linear regimes, separated by a cutoff frequency of about 300 Hz; above the cutoff, the $1/f^2$ noise has been detected in all of the spectra. Below the cutoff, we found a slope higher than 0, with an α exponent close to 1, for regions whose distance from the contact point ranges from 0.25 to 0.75 nm. For higher distances, the power spectra have been found to be practically flat. An example is shown in Figure 5, in which the establishment of $1/f$ noise

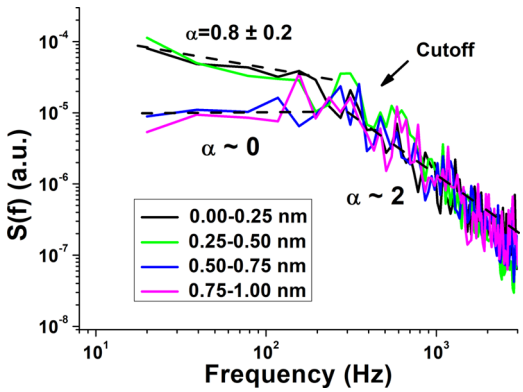

Figure 5. Power spectra of 0.25 nm long regions from the approaching curve located at different distances from the contact point (see the inset); only regions from force curves related to specific events (i.e., showing $1/f$ noise in the 10 nm long regions) have been analyzed. Dashed black lines indicate the best fit through the expression $S(f) \sim 1/f^{\alpha}$, below and above the cutoff frequency of about 300 Hz. The reported α exponents are the average and the corresponding standard deviation as obtained from a collection of 30 curves.

appears at a distance of about 0.50 nm from the contact point. The difference between the α values has also been assessed by a confidence test with a significance level higher than 90%.

By taking into consideration the results from all of the collected regions, we found that $1/f$ noise takes place at an average distance of 0.55 nm with a standard deviation of 0.20 nm. It should be remarked that such a value represents the effective tip−substrate distance because of the use of an AFM equipment with a closed-loop scanner (see the Experimental Section).

By taking into consideration that $1/f$ noise directly reflects a specific biorecognition event, these results indicate the distance between the partners at which biorecognition starts, with this deserving some interest in the perspective to elucidate the involved mechanisms. Under the assumption that the tip switches between a state closer or farther to the substrate, we have analyzed the force fluctuations in the region where biorecognition is active, in terms of a two-state, binary process. In particular, we have defined τ_{close} as the time during which the tip is closer to the substrate with respect to a threshold chosen as the standard deviation of the force in the analyzed interval, roughly corresponding to the baseline. The distribution of τ_{close}, as derived from 30 collected regions corresponding to specific (red circles) and nonspecific (black squares) events, is shown in the semilog plot in Figure 6. The

DOI: 10.1021/acsomega.8b02993
ACS Omega 2019, 4, 3627−3634

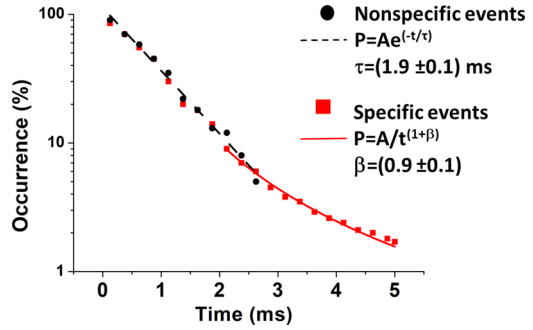

Figure 6. Distribution of the τ_{close} times (see the text) as extracted from the 0.25 nm long regions of the approaching curves, located just before the contact point and related to specific biorecognition events (red squares) or to nonspecific events (black circle). Each distribution has been obtained by taking into consideration data from a collection of 30 regions. Lines are bestfits by the given expressions; the extracted fitting parameters have been reported.

distribution of τ_{close} related to nonspecific events follows a linear trend, which can be well described by an exponential decay with a characteristic time of about 1.9 ms (see the dashed black line). A linear trend, with almost the same slope, has been also detected for the distribution related to specific events for τ_{close} shorter than 2 ms. At variance, for longer times, the distribution of τ_{close} related to specific events exhibits a tail at long times whose trend significantly deviates from the linear one. Indeed, the distribution for time values longer than 2 ms can be well described by a power law distribution $P \sim 1/(t^{\beta+1})$ with $\beta \sim 0.9$ ms (see the continuous red line). These results are reminiscent of those obtained for the biotin−avidin complex, by following a slightly different procedure, from which a slightly lower value ($\beta \sim 0.7$) was obtained.[14]

Generally, the concomitant presence of both the $1/f$ noise and a power law in force fluctuations can be explained in terms of a superposition of independent stochastic signals arising from the diffusive process of the rough energy landscape theory.[23,24] In this connection, it is interesting to note that both the cutoff frequency of the power spectrum and the change of the regime in the τ_{close} distribution indicate that the characteristic times of biorecognition fall in the range of milliseconds, with this also corresponding to the estimated transition times among conformations of biomolecules as emerging from different works.[25,26] On such a basis, our results about the $1/f$ noise and the τ_{close} distribution can be analyzed and discussed in connection with the models describing the biomolecular binding process in terms of the energy landscape exploration. As already mentioned, two main models, CS and IF, are usually invoked to describe the mechanisms underlying the formation of a complex. In the CS model, each biomolecule continuously undergoes transitions between different conformational substrates, binding to the partner when it assumes the most appropriate conformation. In other words, the complex is formed through an optimized fit based on the selection from pre-existing ensemble of conformations. Accordingly, during the approach, the biomolecules are expected to explore different conformations by establishing a biorecognition when appropriate conformations are assumed. On the other hand, in the framework of the IF model, the biomolecule first binds to the partner and then it undergoes conformational changes for optimizing the structure of the complex.

Our results show that $\beta 2\mu$globulin and anti$\beta 2\mu$globulin molecules start to recognize each other at a distance of about 0.50 nm, which is well before their effective binding state. The capability of two partners to recognize each other before reaching a physical contact suggests a rather high affinity between the molecules. This suggests that the biorecognition occurs in correspondence to specific molecular conformations as well as to particular relative arrangements, with a better matching with the CS model. A further support to such a hypothesis comes also from the rather low probability to form a specific complex usually observed in AFS biorecognition experiments.[27] Indeed, even if the formation of a complex in AFS could depend on several factors, such as functionalization, orientation, linker length, etc., a further contribution from the selection of molecules assuming conformations well matching the partner structure could also be invoked.

On the other hand, the appearance of a long tail in the τ_{close} distribution is consistent with a slowing down of the energy landscape exploration during the molecular approaching. This could be due to a conformational reassessment of the biomolecules to optimize the binding to the partner. Such a picture is in correspondence with the IF model in which the biorecognition process guides the biomolecules through a restricted exploration of the energy landscape. On such a basis, the possibility that biorecognition could be a combination of CS and IF binding mechanisms could be speculated, leading to a sort of hybrid CS−IF model. In other words, biorecognition could take place when the biomolecules assume particular molecular conformations and arrangements; some structural refinements may occur successively, even upon binding. Such a picture could also find a correspondence with recent theories for which both the CS and IF mechanisms are active in biorecognition, with the prevalence of one or the other depending on the particular conditions of measurements even in connection with the investigated system.[26,28]

Finally, we discuss the result for the process in which the biorecognition starts when the biomolecules are at a distance of about 0.50 nm, in connection with the properties of surrounding water. We remark that a protein molecule in solution is surrounded by water molecules organized in layers, whose structural and dynamical properties vary with the distance from the molecular surface. The first hydration layer, extending up to about 0.25−0.30 nm from the molecular surface, exhibits peculiar properties, such as anomalous diffusion, power law distribution, etc.[29−31] In particular, the $1/f$ noise has been detected in the energy fluctuations of both a protein (plastocyanin) and its hydration water by molecular dynamics (MD) simulations.[32,33] On such a basis, at a distance of 0.50 nm between the two partners, the corresponding hydration layers are expected to come in contact, with some possible effects on the related protein dynamics and then on the binding process. In this respect, the role played by the hydration water network in biorecognition should be further investigated by performing ad hoc experiments and simulations. For example, it could be proposed to carry out AFS biorecognition experiments using different environmental conditions able to modulate the hydration layer extension (e.g., using different polar solvents or by varying the concentrations of ions). In such a way, possible effects on the distance at which the biomolecular partners start to recognize each other could be evaluated. These results could be integrated with MD simulations to investigate, at the atomic

DOI: 10.1021/acsomega.8b02993
ACS Omega 2019, 4, 3627−3634

level, the molecular mechanisms regulating the interplay between local dynamics and biorecognition.

3. CONCLUSIONS

The analysis of the force fluctuations in an AFS experiment between $\beta 2\mu$globulin and anti$\beta 2\mu$globulin has shown the appearance of $1/f$ noise when the biomolecules are at a distance of about 0.50 nm, before forming a specific complex. Such a finding has allowed us to localize the extension of the region (active region) where the biorecognition process starts to occur. In this region, the distribution of the times that the tip spends close to the substrate exhibits, besides the $1/f$ noise, a power law trend characterized by a long tail. These results, which are clear fingerprints of a complex temporal behavior, can be put into relationship to a slowing down of the energy landscape exploration, consistent with a restricted sampling dynamics of the conformational states driving to the final biding state. Accordingly, the formation of the specific complex during the biomolecular approaching could be described in terms of a sort of hybrid CS−IF model that combines CS and IF binding mechanisms. Furthermore, the dynamics of hydration water network surrounding the biomolecules, whose energy fluctuations were found to exhibit $1/f$ noise, could be hypothesized to play some role in regulating the biorecognition process. Finally, our results from the AFS biorecognition experiment between individual biomolecules confirm that atomic force fluctuations encode a large amount of information, whose decoding could deserve a high interest for a deeper investigation of the mechanisms underlying the formation of a specific complex between biological partners.

4. EXPERIMENTAL SECTION

4.1. Sample Preparation. The substrate and the tip were prepared by following the procedure reported in ref 15. Briefly, the glass slides were cleaned for 5 min in acetone, dried with nitrogen, and then UV-irradiated for 30 min. They were then immersed in a solution of 2% (v/v) 3-aminopropyl-triethoxysilane (APTES) (Acros Organics) in chloroform, incubated for 3 min at room temperature, rinsed in chloroform, and dried with nitrogen.

The slides were subsequently incubated with a solution of 1% glutaraldehyde (Sigma-Aldrich) in Milli-Q water for 3 min at room temperature, rinsed with Milli-Q water, and dried with nitrogen. Fifty microliter of a 1 mg/mL solution of anti$\beta_2\mu$globulin in 50 mM phosphate-buffered saline (PBS), pH 7.5, was poured onto this amine-reactive surface and incubated overnight at 4 °C. The slides were incubated with 1 M ethanolamine to cap nonreacted *N*-hydroxysuccinimide (NHS) groups for 30 min. Finally, they were gently washed with PBS and stored in buffer at 4 °C.

Rectangular silicon nitride cantilevers (Bruker, MSCT-B) were cleaned in acetone for 10 min, dried with a gentle nitrogen flow, and UV-irradiated for 30 min to expose hydroxyl groups. Tips were then immersed in a solution of 2% (v/v) 3-aminopropyl-triethoxysilane (APTES) in chloroform, incubated for 2 h at room temperature, rinsed in chloroform, and dried with nitrogen. Silanized tips were immersed in 1 mM *N*-hydroxysuccinimide−poly(ethylene glycol)−maleimide (NHS−PEG−MAL, MW 1395 Da, 9.5 nm length; Thermo Scientific Inc.) and dissolved in dimethylsulfoxide (DMSO) for 3 h at room temperature. The NHS-ester group at one end of the PEG linker reacts with the amino-silane molecule to form an amide bond; the maleimide group at the other end reacts with the sulfhydryl group of the cysteine residue linked to the NH_2 terminus of proteins. The tips were washed in DMSO to remove the unbound linkers, rinsed with Milli-Q water, dried with nitrogen, and incubated with 50 μL of a 10 μM solution of $\beta_2\mu$globulin in 50 mM PBS, pH 7.5, overnight at 4 °C. The tips were then incubated with 1 M ethanolamine to cap nonreacted NHS groups for 3 min. Finally, they were gently rinsed and stored in buffer at 4 °C. The functionalization of the AFM tip with $\beta_2\mu$globulin without the PEG linker was done by following the same procedure as used for glass slides.

4.2. Atomic Force Spectroscopy Measurements. Force measurements were performed with an Asylum Research MFP-3D atomic force microscope using a closed-loop nanopositioning scanner on all three axes, which allowed us to measure the cantilever deflection without artifacts. Experiments were carried out in buffer using a liquid cell. The effective cantilever spring constants, k_{eff}, whose nominal value was k_{nom} = 0.02 N/m, were determined by the thermal noise method and found in the 0.0183−0.0196 N/m range.[34,35] Two hundred force curves were acquired as a function of the piezodisplacement by setting: (i) an approaching speed, v, of 10 nm/s; (ii) a retraction speed of 1000 nm/s; (iii) a relative trigger of 15 nm to limit at 0.3 nN the maximum contact force exerted by the tip on the protein monolayer; (iv) a ramp size of 150 nm; and (v) an encounter time (the interval between the approaching and retraction stages) of 100 ms. The spatial resolution, Δx, of the approaching stage was about 4×10^{-4} nm, corresponding to a temporal resolution $\Delta t = 4 \times 10^{-5}$ s, as derived from the relationship $\Delta x = v\Delta t$, where v is the above-mentioned approaching speed. Force curves showing, in the retraction stage, a nonlinear trend before the jump-off were further analyzed by following the procedure reported in ref 15. In particular, the nonlinear trend of these curves was fitted to eventually find out the characteristic stretching of the PEG linker, which is assumed to be indicative of a specific interaction.[12,13] Accordingly, 30 force curves over the total curves were attributed to specific events. An unbinding frequency (i.e., the ratio of the number of curves attributed to specific events to that of total curves) of about 15% was registered; such a value is very close to that previously detected for the same system.[17] To further assess that the selected force curves were reliably ascribed to specific unbinding events, blocking experiments were performed by incubating the anti$\beta_2\mu$globulin-functionalized substrate with a solution of free $\beta_2\mu$globulin (30 μM in PBS buffer). After blocking, we found a reduction of the unbinding frequency by about 65%, confirming the specificity of the $\beta 2\mu$globulin and anti$\beta 2\beta$globulin interaction. For comparison, 30 force curves not attributed to specific events were extracted. All of the curves from these two sets were analyzed by the $1/f$ noise-based procedure described below.

4.3. Power Spectrum Analysis. The spectral content of the cantilever fluctuations, detected by the position-sensitive photodetector and arising from the fluctuating forces acting on the cantilever, was analyzed by determining the power spectrum by the Fourier transform of the correlation function according to

$$S(f) = \int_0^T \langle F(0)F(t)\rangle e^{2\pi i f t} \frac{1}{f} dt \quad (1)$$

DOI: 10.1021/acsomega.8b02993
ACS Omega 2019, 4, 3627−3634

where the brackets ⟨ ⟩ indicate the correlation function, f is the frequency, T is the integration time interval, and $F(t)$ is the force expressed as a function of time. More specifically, the force is registered as a function of the piezodisplacement, z, which depends on time through the relationship $z = vt$, where v is the approaching speed. According to the procedure followed in previous works, the power spectrum was calculated by the maximum entropy method through the expression[36,37]

$$S(f) = \left(\frac{1}{\sum_{k=-M/2}^{M/2} b_k \, e^{2\pi i f k}} \right)^2 \quad (2)$$

where M is the number of poles, set to 128. The power spectrum analysis was carried out on force curve regions extending up to 10 nm and located at different parts of the approaching force curves. Force curves exhibiting the $1/f$ noise in the low-frequency portion of the power spectra from the 10 nm long region were attributed to specific biorecognition events and were selected for further analysis. Power spectrum analysis was also performed on 0.25 nm long regions, sampled from the 10 nm long regions.

AUTHOR INFORMATION

Corresponding Author

*E-mail: bizzarri@unitus.it.

ORCID

Anna Rita Bizzarri: 0000-0003-3298-6639

Notes

The authors declare no competing financial interest.

ACKNOWLEDGMENTS

AGV was supported by the NKFIH OTKA FK-128654 grant.

REFERENCES

(1) Nooren, I. M. A.; Thornton, J. M. Diversity of protein-protein interactions. *EMBO J.* **2003**, *22*, 3486−3492.

(2) Wilchek, M.; Bayer, E. A.; Livnah, O. Essentials of biorecognition: The (strept)avidin−biotin system as a model for protein−protein and protein−ligand interaction. *Immunol. Lett.* **2006**, *103*, 27−32.

(3) Boehr, D. D.; Nussinov, R.; Wright, P. E. The role of dynamic conformational ensembles in biomolecular recognition. *Nat. Chem. Biol.* **2009**, *5*, 789−796.

(4) Fenimore, P. W.; Frauenfelder, H.; Magazu', S.; McMahon, B. H.; Mezei, F.; Migliardo, F.; Young, R. D.; Stroe, I. Concepts and problems in protein dynamics. *Chem. Phys.* **2013**, *424*, 2−6.

(5) Frauenfelder, H.; Chen, G.; Berendzen, J.; Fenimore, P. W.; Jansson, H.; McMahon, B. H.; Stroe, I. R.; Swenson, J.; Young, R. D. A unified model of protein dynamics. *Proc. Natl. Acad. Sci. U.S.A.* **2009**, *106*, 5129−5134.

(6) Koshland, D. E., Jr.; Némethy, G.; Filmer, D. Comparison of Experimental Binding Data and Theoretical Models in Proteins Containing Subunits. *Biochemistry* **1966**, 365−385.

(7) Zhou, H. From Induced Fit to Conformational Selection: A Continuum of Binding Mechanism Controlled by the Time scale of Conformational Transitions. *Biophys. J.* **2010**, *98*, L15−L17.

(8) Yang, H.; Luo, G.; Karnchanaphanurach, P.; Louie, T.-M.; Rech, I.; Cova, S.; Xun, L.; Xie, X. S. Protein conformational dynamics probed by single-molecule electron transfer. *Science* **2003**, *302*, 262−266.

(9) Moerner, W. E. Feature article A Dozen Years of Single-Molecule Spectroscopy in Physics, Chemistry, and Biophysics. *J. Phys. Chem. B* **2002**, *106*, 910−927.

(10) Rief, M.; Grubm, H. Force Spectroscopy of Single Biomolecules. *ChemPhysChem* **2002**, *3*, 255−261.

(11) Hinterdorfer, P.; Dufrêne, Y. F. Detection and localization of single molecular recognition events using atomic force microscopy. *Nat. Methods* **2006**, *3*, No. 347.

(12) Bizzarri, A. R.; Cannistraro, S. The application of atomic force spectroscopy to the study of biological complexes undergoing a biorecognition process. *Chem. Soc. Rev.* **2010**, 734−749.

(13) Hinterdorfer, P.; Baumgartner, W.; Gruber, H. J.; Schilcher, K.; Schindler, H. Detection and localization of individual antibody-antigen recognition events by atomic force microscopy. *Proc. Natl. Acad. Sci. U.S.A.* **1996**, *93*, 3477−3481.

(14) Bizzarri, A. R.; Cannistraro, S. $1/f\alpha$ noise in the dynamic force spectroscopy curves signals the occurrence of biorecognition. *Phys. Rev. Lett.* **2013**, *110*, No. 048104.

(15) Bizzarri, A. R.; Cannistraro, S. Antigen-antibody biorecognition events as discriminated by noise analysis of force spectroscopy curves. *Nanotechnology* **2014**, *25*, No. 335102.

(16) Zheng, G.; Gao, X. P. A.; Lieber, C. M. 2010 Subthreshold regime has the optimal sensitivity for nanowire FET biosensors. *Nano Lett.* **2010**, 3179−3183.

(17) Coppari, E.; Santini, S.; Bizzarri, A. R.; Cannistraro, S. Kinetics and binding geometries of the complex between beta2-microglobulin and its antibody: An AFM and SPR study. *Biophys. Chem.* **2016**, *211*, 19−27.

(18) Parham, P.; Ohta, T. Population biology of antigen presentation by MHC class I molecules. *Science* **1996**, 67−74.

(19) Coppolino, G.; Bolignano, D.; Rivoli, L.; Mazza, G.; Presta, P.; Fuiano, G. Tumour markers and kidney function: a systematic review. *BioMed Res. Int.* **2014**, 1−9.

(20) Cappella, B.; Kappl, M. Force measurements with the atomic force microscope: Technique, interpretation and applications. *Surf. Sci. Rep.* **2005**, *59*, 1−152.

(21) Weissman, M. B. 1/F Noise and Other Slow, Nonexponential Kinetics in Condensed Matter. *Rev. Mod. Phys.* **1988**, *60*, 537−571.

(22) Shlesinger, M. *Lévy Flights and Related Topics in Physics*; Springer-Verlag: Berlin, 1995.

(23) Eliazar, I.; Klafter, J. A unified and universal explanation for Levy laws and 1/f noises. *Proc. Natl. Acad. Sci. U.S.A.* **2009**, *106*, 12251−12254.

(24) Lutz, E. Power-Law Tail Distributions and Nonergodicity. *Phys. Rev. Lett.* **2004**, 1−4.

(25) Chakrabarti, K. S.; Agafonov, R. V.; Pontiggia, F.; Otten, R.; Higgins, M. K.; Schertler, G. F. X.; Oprian, D. D.; Kern, D. Conformational Selection in a Protein-Protein Interaction Revealed by Dynamic Pathway Analysis Article Conformational Selection in a Protein-Protein Interaction Revealed by Dynamic Pathway Analysis. *Cell Reports* **2016**, *14*, 32−42.

(26) Paul, F.; Weikl, T. R. How to Distinguish Conformational Selection and Induced Fit Based on Chemical Relaxation Rates. *PLoS Comput. Biol.* **2016**, 1−17.

(27) Bizzarri, A. R. A. R.; Cannistraro, S. Atomic Force Spectroscopy in Biological Complex Formation: Strategies and Perspectives. *J. Phys. Chem. B* **2009**, *113*, 16449−16464.

(28) Vogt, A. D.; Di Cera, E. Conformational Selection Is a Dominant Mechanism of Ligand Binding. *Biochemistry* **2013**, 5723−5729.

(29) Smith, J. C.; Merzel, F.; Bondar, A. N.; Tournier, A.; Fischer, S.; Kornyshev, A.; Daniel, R. M.; Halle, B.; Wilson, K. Structure, dynamics and reactions of protein hydration water. *Philos. Trans. R. Soc., B* **2004**, *359*, 1181−1190.

(30) Bizzarri, A. R.; Cannistraro, S. Molecular dynamics of water at the protein-solvent interface. *J. Phys. Chem. B* **2002**, *106*, 6617−6633.

(31) Bizzarri, A. R.; Paciaroni, A.; Cannistraro, S. Glasslike dynamical behavior of the plastocyanin hydration water. *Phys. Rev. E* **2000**, *62*, 3991−3999.

(32) Bizzarri, A. R.; Cannistraro, S. Flickering noise in the potential energy fluctuations of proteins as investigated by MD simulation. *Phys. Lett. A* **1997**, *236*, 596−601.

DOI: 10.1021/acsomega.8b02993
ACS Omega 2019, 4, 3627−3634

(33) Carlini, P.; Bizzarri, A. R.; Cannistraro, S. Temporal fluctuations in the potential energy of proteins: 1/f(alpha) noise and diffusion. *Phys. D* **2002**, *165*, 242−250.
(34) Hutter, J. L.; Bechhoefer, J. Calibration of atomic-force microscope tips. *Rev. Sci. Instrum.* **1993**, *64*, 1868−1873.
(35) Sader, J. E.; Sanelli, J. A.; Adamson, B. D.; Monty, J. P.; Wei, X.; Crawford, S. A.; Friend, J. R.; Marusic, I.; Mulvaney, P.; Bieske, E. J. Spring constant calibration of atomic force microscope cantilevers of arbitrary shape. *Rev. Sci. Instrum.* **2012**, *83*, 1−16.
(36) Press, W. H.; Teukolsky, S. A.; Vetterling, W. T.; Flannery, B. P. *Numerical Recipes in C*, 2nd Ed.; Cambridge University Press: Cambridge, U.K., 1992.
(37) Hegger, R.; Kantz, H.; Schreiber, T. Practical implementation of nonlinear time series methods: The TISEAN package. *Chaos* **1999**, *9*, 413−435.

DOI: 10.1021/acsomega.8b02993
ACS Omega 2019, 4, 3627−3634